Computational Study of the Aminolysis of Anhydrides: Effect of the Catalysis to the Reaction of Succinic Anhydride with Methylamine in Gas Phase and Nonpolar Solution

Tetyana Petrova,[†,‡] Sergiy Okovytyy,[†,‡] Leonid Gorb,[†] and Jerzy Leszczynski*[,†]

Department of Chemistry, Computational Center for Molecular Structure and Interactions, Jackson State University, 1400 J.R. Lynch Street, P.O. Box 17910, Jackson, Mississippi 39217-0510, and Department of Organic Chemistry, Dnepropetrovsk National University, Dnepropetrovsk 49625, Ukraine

Received: October 24, 2007; Revised Manuscript Received: March 12, 2008

Different possible pathways of the aminolysis reaction of succinic anhydride were investigated by applying high level electronic structure theory, examining the general base catalysis by amine and the general acid catalysis by acetic acid, and studying the effect of solvent. The density functional theory at the B3LYP/6−31G(d) and B3LYP/6−311++G(d,p) levels was employed to investigate the reaction pathways for the aminolysis reaction between succinic anhydride and methylamine. The single point ab initio calculations were based on the second-order Møller−Plesset perturbation theory (MP2) with 6−31G(d) and 6−311++G(d,p) basis sets and CCSD(T)/6−31G(d) level calculations for geometries optimized at the B3LYP/6−311++G(d,p) level of theory. A detailed analysis of the atomic movements during the process of concerted aminolysis was further obtained by intrinsic reaction coordinate calculations. Solvent effects were assessed by the polarized continuum model method. The results show that the concerted mechanism of noncatalyzed aminolysis has distinctly lower activation energy compared with the addition/elimination stepwise mechanism. In the case of the process catalyzed by a second methylamine molecule, asynchronous proton transfer takes place, while the transition vectors of the acid-catalyzed transition states correspond to the simultaneous motion of protons. The most favorable pathway of the reaction was found through the bifunctional acid catalyzed stepwise mechanism that involves formation of eight-membered rings in the transition state structures. The difference between the activation barriers for the two mechanisms averages 2 kcal/mol at various levels of theory.

Introduction

The aminolysis of anhydrides is an important organic reaction considered as a model for the interaction of a carbonyl group with nucleophiles as well as aminolysis of esters. The reaction can also be viewed as a model process for the formation of peptide bonds. There are numerous kinetic and theoretical studies on ester aminolysis.[1–11]

Earlier, several possible reaction pathways of aminolysis for esters as well as for anhydrides have been discussed. However, there is not enough experimental data for the conclusive assessment of the studied phenomena. All of the discussed data conform to the available kinetic results. As has been noted before, there is much less experimental data on aminolysis of anhydrides than for esters, while they have common mechanisms in many respects. Three principle schemes have been considered in both cases:[12,13] a stepwise mechanism through zwitterionic intermediates; a stepwise path through neutral intermediates; and a concerted pathway involving simultaneous cleavage of the C−O single bond and formation of a C−N bond. Jencks and co-workers studied the catalytic influences of solvents such as water and general base catalysis by the amine, and general acid catalysis by the protons, carboxylic acids, and ammonium ions as well as the overall influence of the media and pH for ester aminolysis.[2–4,14–17]

Advanced electronic structure theory studies of the reaction are able to facilitate the selection of the most feasible mechanism of reaction among the different possibilities.[12,18–21] Yang and Drueckhammer studied the aminolysis of ethyl thioacetate by applying the MP2/6−31+G(d) and MP2/6−31G(d,p) levels of theory.[12] Their results support a stepwise mechanism through neutral intermediates involving water-catalyzed proton transfer. The theoretical results show similar values of activation energy for the stepwise and the concerted pathways. The obtained differences in activation energies for the two mechanisms were revealed after considering the specific catalytic role of the water solvent.

Reliable computational studies of aminolysis of esters and anhydrides had started in the 1990s. In 1996, Zipse et al. studied the mechanism of the reaction of methyl acetate with methylamine by applying the HF/3−21G and HF/6−31G(d,p) levels of theory.[20,21] They showed that the quantum chemical calculations favor a stepwise addition/elimination pathway over the direct substitution mechanism.[22]

In another study, Houk and co-workers[20] also evaluated the effects of catalysts on the energy profile of the reaction. The authors found that the difference in energies for the transition states along the two alternatively considered pathways is minimal. The activation energy predicted at the HF/6−31G(d,p) level was 42.1 kcal/mol for the concerted mechanism and 41.8 kcal/mol for the stepwise mechanism.

Another mechanism, a fully stepwise pathway, has also been studied. Oie and co-workers[22] and Zipse and co-workers[20] studied a fully stepwise pathway through zwitterionic intermediates; however, they have not located transition states associated with these zwitterionic intermediates. Moreover, later studies at the MP2/6−31G(d,p) levels of theory carried out by Ilieva and co-workers[13] for the reaction of methylformate and me-

* Author to whom correspondence should be addressed. E-mail: jerzy@ccmsi.us.
† Jackson State University.
‡ Dnepropetrovsk National University.

10.1021/jp7102897 CCC: $40.75
Published on Web 05/21/2008

SCHEME 1: Schematic Representation of Possible Mechanisms of the Uncatalyzed Aminolysis Reaction

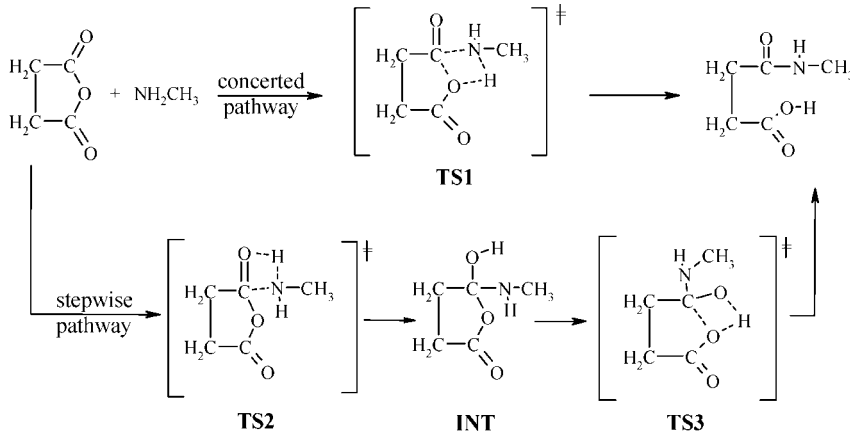

thylamine also failed to identify zwitterionic transition states and intermediates. Also Singleton and Merrigan[23] using the density functional theory at the B3LYP/6−31G(d,p) level investigated the formation of zwitterion between methyl formate and ammonia and hydrazine in a water medium. They calculated various solvated structures involving from 4 to 11 explicit water molecules. However, no effort was made to find global minima for these structures. The focus of the study of Singleton and Merrigan[23] was to explain the kinetic isotope effect data for the aminolysis reaction, obtained earlier by Marlier and co-workers.[24]

The concerted and neutral stepwise mechanisms of aminolysis of methyl formate with ammonia have been investigated by Ilieva and co-workers at the B3LYP/6−31G(d) and QCISD/6−31G(d,p) levels of theory.[13] Their results reveal that the rate-determining steps along the concerted and stepwise pathways involve proton transfers. In the case of uncatalyzed aminolysis, B3LYP/6−31G(d) calculations predict the stepwise mechanism to be more favorable than the concerted pathway. In the gas phase, the activation barrier for the stepwise mechanism is lower by 2.0 kcal/mol than for the concerted mechanism. The higher level quantum mechanical computations bring closer the energy barriers for the concerted and stepwise mechanisms of aminolysis studied (to 46.7 and 44.8 kcal/mol, respectively). In the case of ester aminolysis, the barrier was earlier found to result mainly from unfavorable proton transfer geometries.[21] In the study of Ilieva and co-workers, the calculations reveal the stepwise mechanism of the catalyzed reaction to be more favorable by 7.4 kcal/mol.[13]

The acetylation of methanol and methylamine with acetic anhydride was investigated by Kruger.[25] He applied the gas phase calculation using the RHF, B3LYP, and MP2 approaches with the 6−31+G(d, p) basis set. A six-membered cyclic transition state of acetic anhydride with a reagent was found, thereby indicating that the reaction occurs as a concerted process in which acetyl formation and the loss of a proton from the alcohol oxygen or amine nitrogen atom occurs simultaneously. The geometries of the transition states correspond well with those for the hydrolysis of acetic anhydride with water found by Yamabe and Ishikawa.[26] Similar transition states were found with *tert*-butyl dicarbonate (T-Boc) anhydride as well as for the secondary amines.[25]

The analysis of previous works shows that the reaction pathways have been treated in detail for many different pairs of reagents. However, for the aminolysis of cyclic anhydride, the present calculations provide the first comprehensive quantitative theoretical results that include the reaction pathways and the energy barriers. The present report is devoted to the investigations of the possible pathways for the anhydride aminolysis reaction by applying high levels of electronic structure theory and studying the solvent effects. In addition, the base catalysis of the reaction by methylamine and acid catalysis by acetic acid have also been considered. The model reaction of succinic anhydride and methylamine is studied in the gas phase and in the nonpolar solution. We selected benzene as a neutral, aprotic solvent, which is used for aminolysis of anhydrides in organic synthesis[27,28] and is not expected to have a catalytic effect. Kinetic investigations of the aminolysis reaction in benzene also have been carried out for the interaction between benzylamine and succinic anhydride by Smagowski and Bartnicka.[29] An autocatalytic type of the reaction has been ascertained. An application of aprotic organic solvent is also essential for biochemical investigations of processes, for example, reversibly inactivating thermostable DNA polymerase or ligase by dicarboxylic acid anhydride wherein the reaction with anhydride was carried out using a dried DNA polymerase or ligase in an anhydrous aprotic organic solvent.[30]

Computational Methods

The computations were carried out with the Gaussian 03 program package at the B3LYP, MP2, and CCSD(T) levels of theory. Geometry optimizations of the local minima and transition state structures were carried out at the B3LYP/6−31G(d) and B3LYP/6−311++G(d,p) levels of theory. The geometry of the local minima and transition states has been verified by establishing that the matrices of the energy second derivatives (Hessians) at the B3LYP/6−31G(d) level have zero and one negative eigenvalues, respectively. Single point energy evaluations were also performed at the MP2/6−31G(d), MP2/6−311++G(d,p), and CCSD(T)/6−31G(d) levels of theory for structures, corresponding to critical points on the potential energy surface, optimized at the B3LYP/6−311++G(d,p) level. The total energies calculated at the B3LYP, MP2, and CCSD(T) levels have been corrected for the B3LYP/6−31G(d) level zero-point energies scaled by a factor of 0.9806.[31] The thermal and entropic contributions to the free energies were taken from the B3LYP/6−31G(d) frequency calculations.

The computed enthalpy, entropy, and Gibbs free energy were converted from 1 atm standard state into the standard state of molar concentration (ideal mixture at 1 mol per liter and 1 atm) in order to allow a direct comparison with the experimental result in solution.[32]

For a concerted mechanism of reaction, the intrinsic reaction coordinate (IRC) computations[33] at the B3LYP/6−31G(d) level

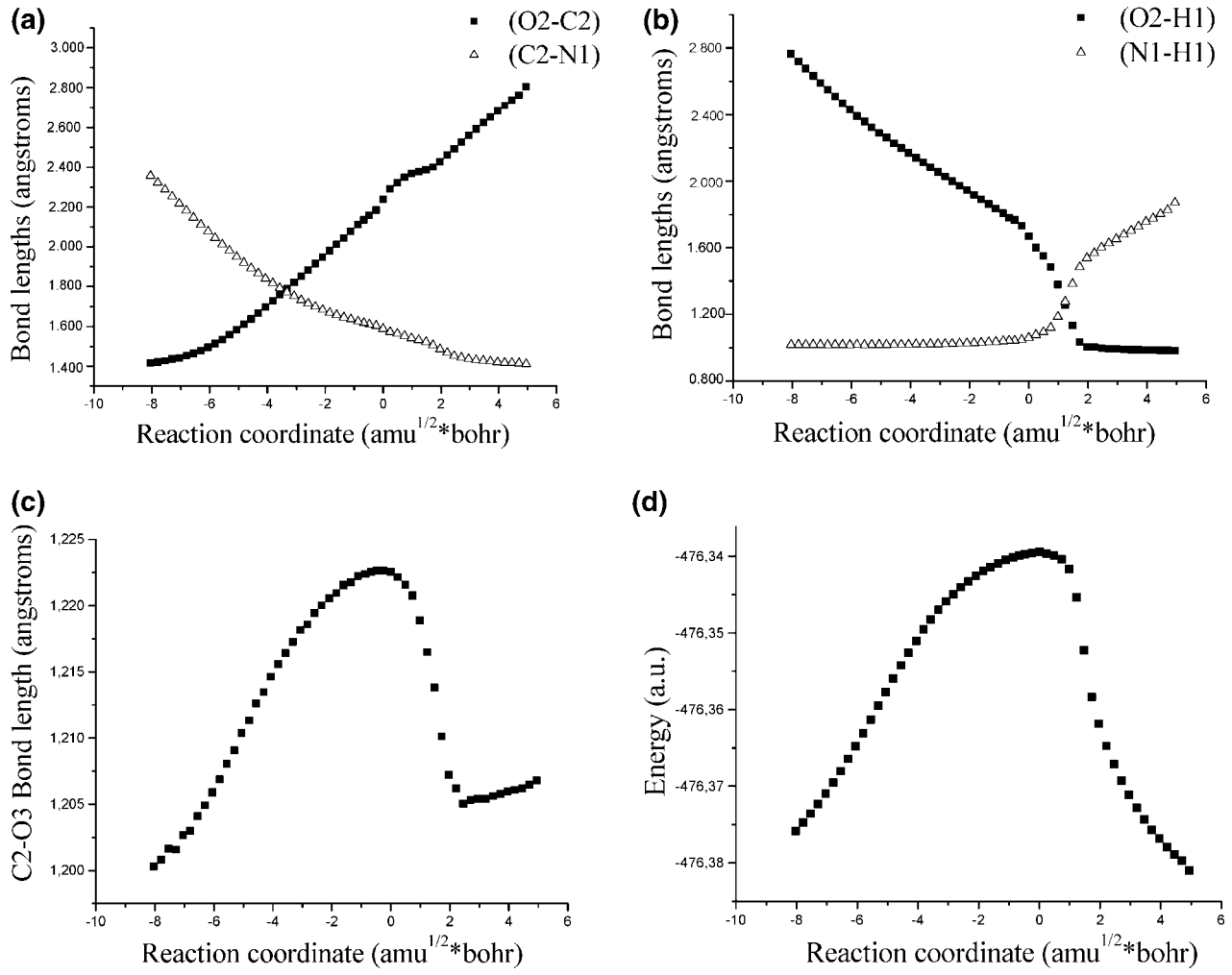

Figure 1. Evolution of the bond lengths (a−c) and energy changes (d) along the IRC for the concerted mechanism of uncatalyzed aminolysis of succinic anhydride by methylamine at the B3LYP/6−31G(d) level of theory.

of theory were used to follow the paths leading from transition state to the two minima associated with it, thus confirming the connection of two minima and one saddle point. The intrinsic reaction coordinate was traced by solving the IRC equation with an algorithm developed by Gonzales and Schlegel[34] and incorporated into DFT-based schemes by Deng and Ziegler.[35]

Polarizable continuum model (PCM)[36] B3LYP/6−31G(d) optimization calculations were performed for estimation of the change in geometry and energetics of the reaction in the presence of a nonpolar aprotic solvent. The dielectric constant ($\varepsilon = 2.247$) which formally corresponds to the bulk of benzene has been used.

Results and Discussion

Uncatalyzed Aminolysis. To sum up all previous discussed results, the most likely schemes for the aminolysis reaction have been determined. These schemes were explored in our study for the reaction of succinic anhydride with methylamine. We use the term "uncatalyzed" for the processes which do not involve additional molecules of catalyst consumed itself by the overall reaction. According to the results obtained, two possibilities were considered: the concerted and neutral stepwise mechanisms. The mechanism of the attack is different in these two cases. In contrast to calculations in water medium, where we have found a zwitterionic transition state and intermediate ($\Delta E^{\ddagger} = 4.81$ kcal/mol, PCM/B3LYP/6−31G(d)), all attempts to identify a zwitterionic mechanism in the gas phase and benzene failed. Since this paper focuses on quantitative analysis of the aminolysis reaction in gas phase and in the presence of the nonpolar solvent (benzene), we will defer discussion of solvent effects of water to a future report (see Supporting Information).

For the concerted pathway, the reaction consists of one step, in which all bond-forming and bond-breaking processes occur in concert (Scheme 1). The anhydride aminolysis reaction usually starts with the formation of a substrate−nucleophile complex. In the case of a concerted mechanism, a proton from the methylamine molecule is transferred to the anhydride oxygen atom simultaneously with a nucleophilic methylamine molecule attack on the electrophilic carbon atom of the anhydride. Thus, the transition state for the concerted mechanism (**TS1**) involves formation of a C2−N1 bond, cleaving of the anhydride C2−O2 bond, and a proton transfer from the methylamine toward the oxygen. Computational data, namely, the values of bond lengths in the **TS1**, are presented in Figure 2 (cartesian coordinates for B3LYP/6−31G(d), B3LYP/6−311++G(d,p), and PCM/B3LYP/6−31G(d) (solvent−benzene) fully optimized geometries of the reagents, prereactive complexes, transition states, and intermediates are given in Supporting Information).

Because of the large structural differences between transition state (**TS1**), reactants, and product, the transition structure for the concerted mechanism of reaction was investigated by

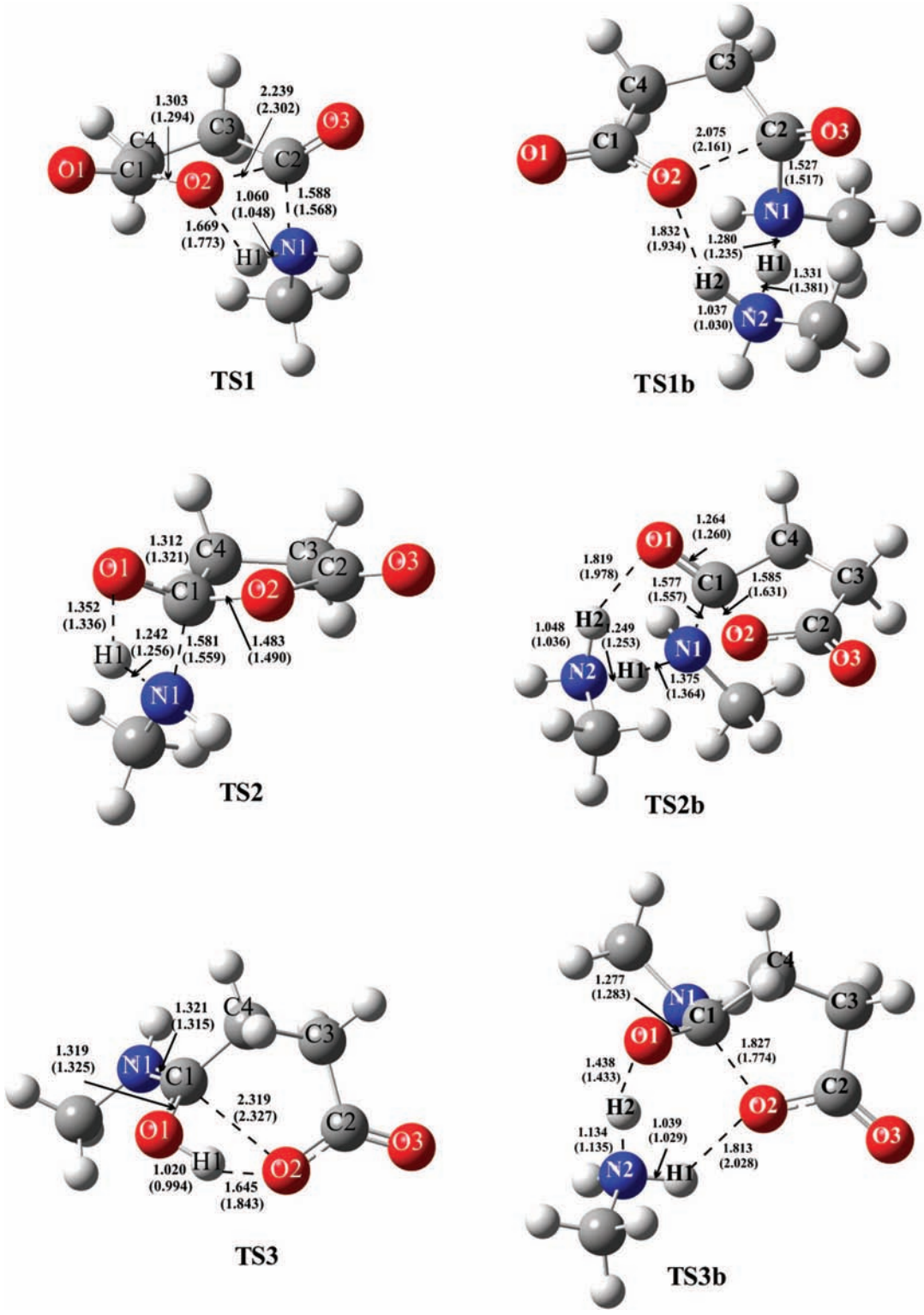

Figure 2. Geometrical parameters of transition states along the concerted and stepwise pathways for the uncatalyzed (**TS1-TS3**) and catalyzed by the methylamine (**TS1b-TS3b**) aminolysis of succinic anhydride optimized at the B3LYP/6−31G(d) and PCM/B3LYP/6−31G(d) (in parentheses) levels of theory.

intrinsic reaction coordinate computations at the B3LYP/6−31G(d) level of theory. IRC calculations for the two directions from the transition state (**TS1**) show that this structure converts to a prereactive complex and product of reaction, respectively (Figure 1). It seemed pertinent to study this pathway in some detail.

Analysis of the reaction trajectory reveals two major processes: first, rupture of the anhydride C2−O2 bond and, second, proton migration. The overall reaction profile via this transition structure is consistent with the asynchronous concerted rearrangement elaborated below.

Figure 1 provides a detailed description of the atomic motion during the course of the aminolysis process. The reaction can essentially be described by three internal modes of transformation. The first one is the O2−C2 bond stretch eventually leading to the breaking of the O2−C2 σ bond. The second mode

involves the formation of the single bond between the C2 atom of anhydride and the N1 nitrogen atom of methylamine, which can be followed based on changes in the C2−N1 bond length (Figure 1a). The third mode is a transfer of a hydrogen atom: H1 migrates from the N1 atom of the attacking methylamine molecule to the O2 atom of the succinic anhydride. This mode is characterized by N1−H1 and H1−O2 bond lengths (Figure 1b).

It is clear from the displayed plots (Figure 1a,b) that the geometrical parameters do not change gradually and simultaneously as the reaction proceeds. The first phase, the rupture of the anhydride ring and the C2−N1 bond formation, is followed by a second phase, H1 proton migration. The combination of these two phases defines a concerted asynchronous pathway. It follows from Figure 1 that the C2−O2 and C2−N1 bond lengths smoothly change during the reaction, while the O2−H1 and N1−H1 bonds undergo remarkable changes in the interval of 0.0−0.2 amu$^{1/2}$ Bohr. The length of the C2−O1 double bond does not change significantly, while the O3−C2 bond is increased from 1.200 Å to 1.223 Å (at −0.242 amu$^{1/2}$ Bohr, Figure 1c) and then shortens back to 1.207 Å (at 4.950 amu$^{1/2}$ Bohr). Figure 1d displays the energy changes along the IRC.

The second possibility for the reaction mechanism is a stepwise pathway, which could be characterized as an addition/elimination mechanism, in which the addition and elimination steps are coupled with the proton transfer to retain neutrality in the tetrahedral intermediate that is formed (Scheme 1). The reaction starts with the attack of the N1 atom from methylamine on the C1 atom in the anhydride molecule. The transition state for this stage (**TS2**) along the reaction coordinate (Figure 2) possesses a tetrahedral carbon atom. The C2−N1 bond is almost formed (1.575 Å), while the C1−O1 bond is characterized by a bond length intermediary that is between a double bond and a single bond (1.314 Å). The imaginary vibration vector for the transition state of the first step (**TS2**) (see Supporting Information) corresponds mostly to a proton transfer from the nitrogen atom N1 toward the oxygen atom O1. This stage results in the formation of the stable intermediate **INT**, in which the C1−N1 bond is formed (1.447 Å). There are no minima on the potential energy surface which correspond to the addition of a methylamine molecule to the anhydride without proton transfer. The proton is already transferred to form a hydroxyl group, and the carbonyl carbon atom becomes a tetrahedral center. All geometrical parameters are given at the B3LYP/6−311++G(d,p) level of theory.

The second stage of the process includes breaking of the C1−O2 anhydride single bond and the simultaneous restoration of the C1═O1 bond after the proton transfer between the two oxygen atoms. The transition state vector of the second step **TS3** (see Supporting Information) indicates a proton transfer and a recovering of the C1═O1 double bond character. In the **TS3** structure, the C1−O2 single bond is almost broken (2.351 Å at B3LYP/6−311++G(d,p)). Optimization of the geometry for **TS3** following the transition vector leads to the formation of the product of the reaction.

The calculated values of the activation energy ($\Delta E^{\ddagger}$), enthalpy ($\Delta H^{\ddagger}$), entropy ($\Delta S^{\ddagger}$), and activation Gibbs free energy ($\Delta G^{\ddagger}$) relative to the reactants for the fully optimized critical structures along both concerted and stepwise uncatalyzed pathways are given in Table 1. It can be seen from Table 1 and Figure 5 that in the case of the stepwise mechanism the first stage of the reaction is rate-determining. It is also necessary to state that the calculations predict the concerted mechanism to be more favorable than the stepwise pathway.

TABLE 1: Values of Zero-Point Corrected Activation Energy ($\Delta E^{\ddagger}$), Enthalpy ($\Delta H^{\ddagger}$), Gibbs Free Energies ($\Delta G^{\ddagger}$, kcal/mol), and Entropy ($\Delta S^{\ddagger}$, cal/(mol K)) for the Concerted and Stepwise Mechanisms of Uncatalyzed and Base Catalyzed Aminolysis of Succinic Anhydride by Methylamine

		concerted mechanism[a]	stepwise mechanism		concerted mechanism[a]	stepwise mechanism	
computational level		(Reactants→TS1)	step I[a] (Reactants→TS2)	step II (Intermediate→TS3)	(Reac tants→TS1b)	step I[a] (Reactants→TS2)	step II (Intermediate→TS3)
B3LYP/6−31G(d)	$\Delta E^{\ddagger}$	24.66	34.29	16.23	3.86	6.11	11.39
	$\Delta H^{\ddagger}$	24.39	33.84	16.91	4.00	5.89	12.27
	$\Delta S^{\ddagger}$	−36.11	−37.43	10.61	−65.25	−68.57	14.64
	$\Delta G^{\ddagger}$	35.15	45.00	13.75	23.45	26.34	7.91
	$\Delta\Delta^{b}$	10.49	10.71	−2.49	19.60	20.24	−3.48
B3LYP/6−311++G(d, p)	$\Delta E^{\ddagger}$	24.60	36.10	12.91	7.66	11.28	10.02
	$\Delta G^{\ddagger c}$	35.09	46.81	10.42	27.26	31.52	6.55
MP2/6−31G(d)//B3LYP/6−311++G(d, p)	$\Delta E^{\ddagger}$	20.87	29.85	21.23	−2.61	−1.70	12.61
	$\Delta G^{\ddagger c}$	31.36	40.56	18.74	16.98	18.54	9.14
MP2/6−311++G(d, p)// B3LYP/6−311++G(d, p)	$\Delta E^{\ddagger}$	20.47	28.39	20.47	−1.23	0.09	13.10
	$\Delta G^{\ddagger c}$	31.45	39.10	17.98	18.37	20.32	9.62
CCSD/6−31G(d)//B3LYP/6−311++G(d, p)	$\Delta E^{\ddagger}$	25.26	34.52	22.26	4.64	6.24	16.73
	$\Delta G^{\ddagger c}$	35.75	45.23	19.77	24.24	26.47	13.26
CCSD(T)/6−31G(d)// B3LYP/6−311++G(d, p)	$\Delta E^{\ddagger}$	22.6	32.12	21.10	0.87	2.23	14.49
	$\Delta G^{\ddagger c}$	33.09	42.83	18.61	20.46	22.46	11.02
PCM/B3LYP/6−31G(d)	$\Delta E^{\ddagger}$	17.86	33.03	11.71	0.17	3.37	9.61
	$\Delta H^{\ddagger}$	19.64	32.58	12.47	2.48	5.41	5.19
	$\Delta S^{\ddagger}$	−35.60	−37.03	11.77	−63.75	66.99	9.45
	$\Delta G^{\ddagger}$	30.25	43.62	8.95	21.49	25.39	5.19

[a] Activation parameters have been calculated relative to isolated reactants. [b] ΔΔ−The differences between ΔE and ΔG were derived with the B3LYP/6-311G(d) method and applied to all computational methods. [c] The zero-point corrections as well as the thermal and entropic contributions to the free energies were taken from the B3LYP/6−31G(d) frequency calculations (ΔΔ).

SCHEME 2: Schematic Representation of Possible Mechanisms of the Base Catalyzed Aminolysis Reaction

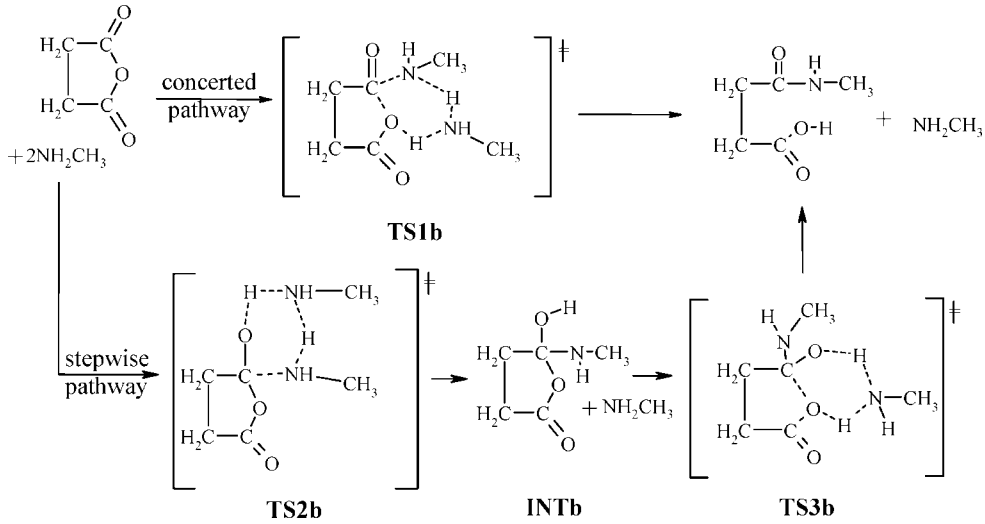

General Base-Catalyzed Aminolysis. The next step in this computational study is to investigate the catalytic effect of methylamine and acetic acid for two considered mechanisms for anhydride aminolysis. According to experimental observations, the reaction can take place as a catalyzed process with the catalytic involvement of the second amine molecule or bifunctional catalysis with a carboxylic acid arising together with the amide from the reaction between the anhydride and the amine which manifests itself frequently in an S-shaped transformation curve.[29]

From the results obtained for the base catalyzed aminolysis reaction, one can see that the concerted mechanism as well as the rate-determining step along the stepwise pathway involves proton transfers through six-membered cyclic transition states

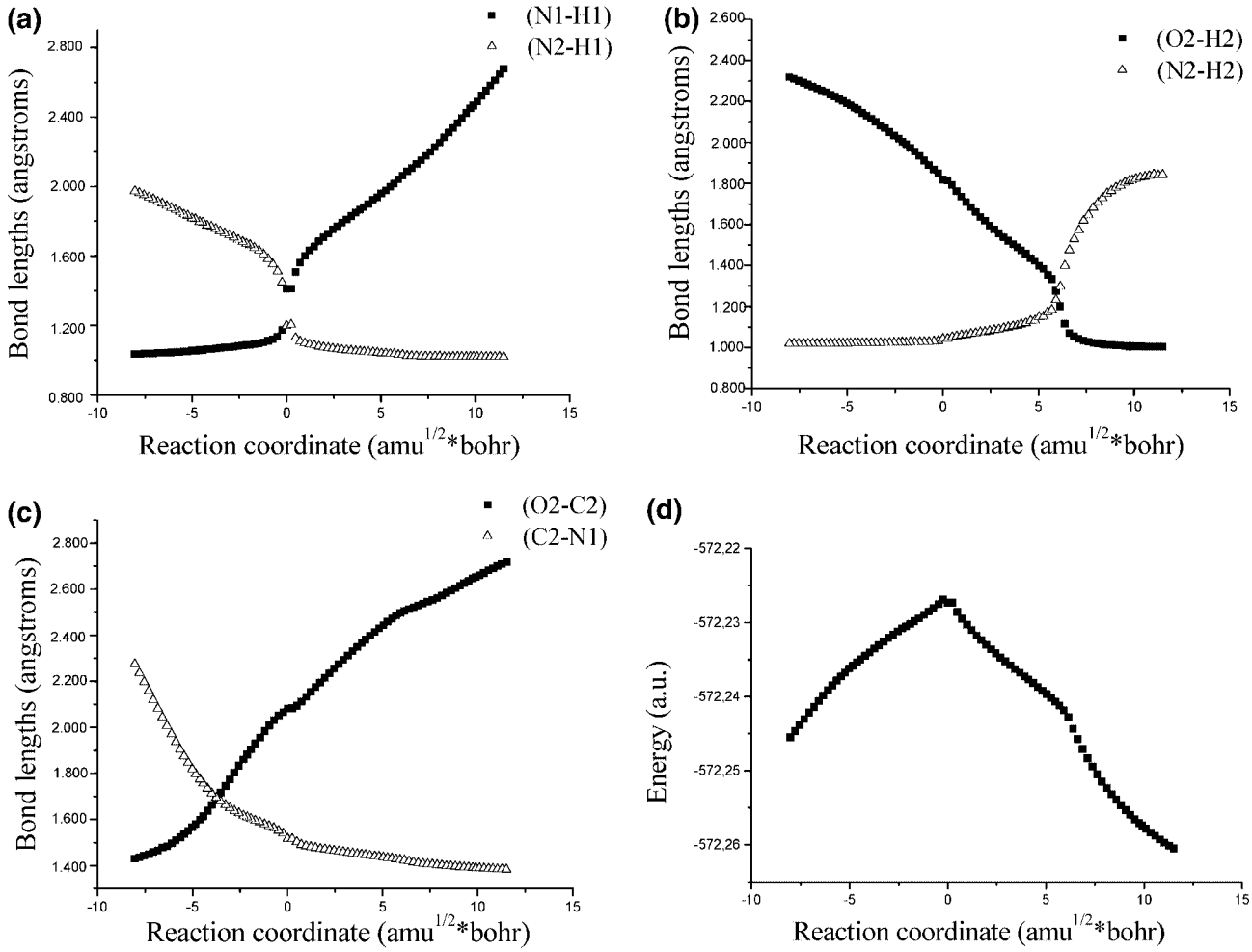

Figure 3. Evolution of bond lengths (a−c) and energy changes (d) along the IRC for the concerted mechanism of catalyzed aminolysis of succinic anhydride by methylamine at the B3LYP/6−31G(d) level of theory.

SCHEME 3: Schematic Representation of Possible Mechanisms of the Acid Catalyzed Aminolysis Reaction

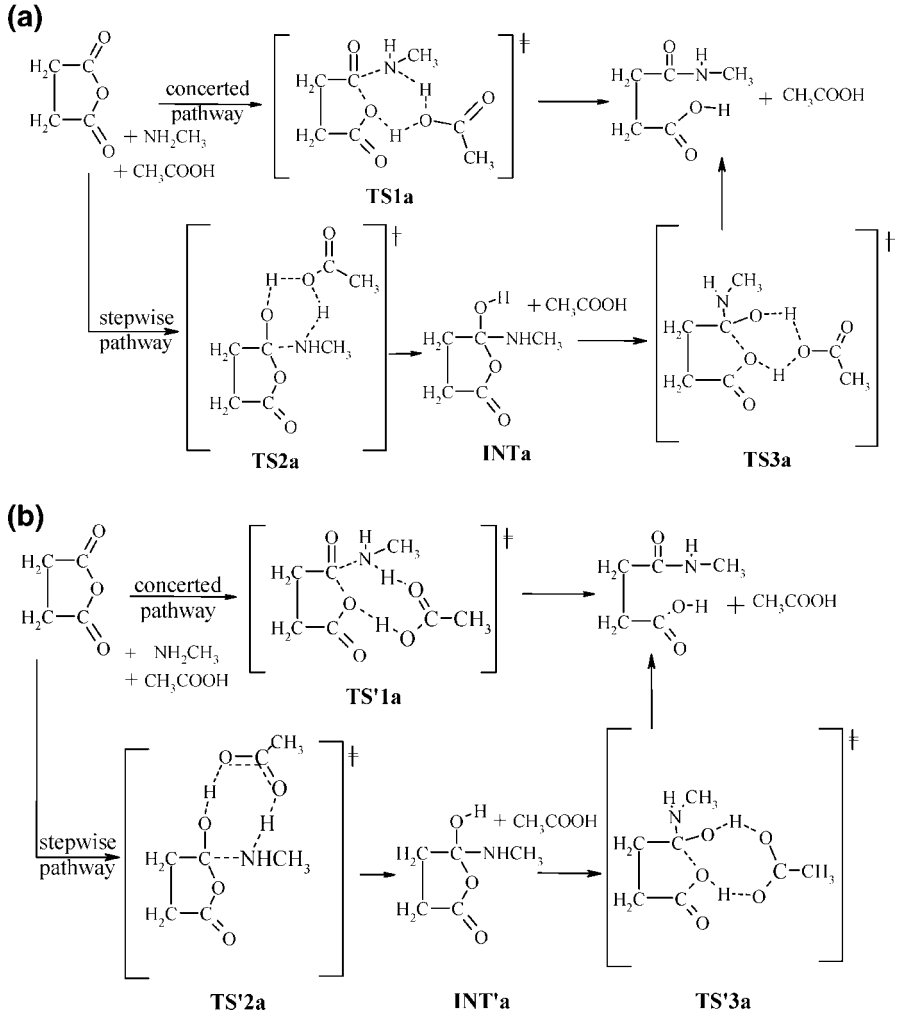

(Scheme 2). These structures are characterized by less ring strain than four-membered rings in the case of uncatalyzed reaction. In other words, the role of the catalyst in the process is to facilitate the proton transfer, thus lowering the proton-transfer energy barrier. The structures of the transition state (**TS1b**) along the concerted mechanism as well as the transition states (**TS2b**, **TS3b**) along the stepwise catalyzed aminolysis of succinic anhydride with a second catalytic methylamine molecule are presented in Figure 2. The activation parameters along the reaction profiles are represented in Table 1.

As can be seen from the structure of **TS1b** (Figure 2), the second methylamine molecule plays a catalytic role in the proton transfer process. Formally, one of the methylamine molecules could be designated as the nucleophilic agent in the process while the second methylamine serves as the catalyst.

The transition vector of **TS1b** (see Supporting Information) represents basically the H1 proton transfer from the nucleophilic methylamine molecule to the catalytic methylamine molecule. Their structures and the existing intermolecular hydrogen bonds are shown in Figure 2.

The IRC of the ring-opening process was studied at the B3LYP/6−31G(d) level. An examination of the reaction intrinsic coordinate along both reactants and products shows the existence of a prereactive complex and product. The plots of the changes in the IRC path are shown in Figure 3a−c. The corresponding energy profile is displayed in Figure 3d. It follows from Figure 3 that the transition state **TS1b** is connected by the steepest descent path to the prereactive complex and the product of the reaction. The calculation progressed sufficiently in each direction to establish this concerted asynchronous pathway between them.

A detailed analysis of IRC in the case of catalyzed aminolysis shows that the motions of the atoms have the same character as for the uncatalyzed process. Thus, O2−C2 and C2−N1 bond changes describe the breaking of the O2−C2 σ bond and the formation of the C2−N1 σ bond. It is of interest to distinguish two cases of concerted proton transfers: H1 migrates from the N1 atom of the attacking nucleofile to the N2 atom of the catalytic methylamine molecule (see N1−H1 and N2−H1 bond lengths, Figure 3a), while H2 migrates from the N2 to the O2 atom (see N2−H2 and O2−H2 bond lengths, Figure 3b). It is also necessary to state that in this case a consecutive proton transfer takes place at 0.0 amu$^{1/2}$ Bohr (H1 proton migrates from N1 of the attacking nucleophile to the N2 atom of the catalytic methylamine molecule, Figure 3a), while the H2 proton migrates from the N2 to the O2 atom at 5.5 amu$^{1/2}$ Bohr (Figure 3b). The change of bond lengths in Figure 3a,b indicates further that transfer of the H1 and H2 protons takes place after the O2−C2 bond breaking and the C2−N1 bond forming reactions.

Similar to the uncatalyzed process, the attack takes place along the C1═O1 carbonyl bond (Scheme 2). The transition state for the first stage (**TS2b**) is characterized by the formation of a C1−N1 bond. The transition vector clearly indicates that the proton-transfer processes take place during this step (see Supporting Information). The catalytic methylamine molecule

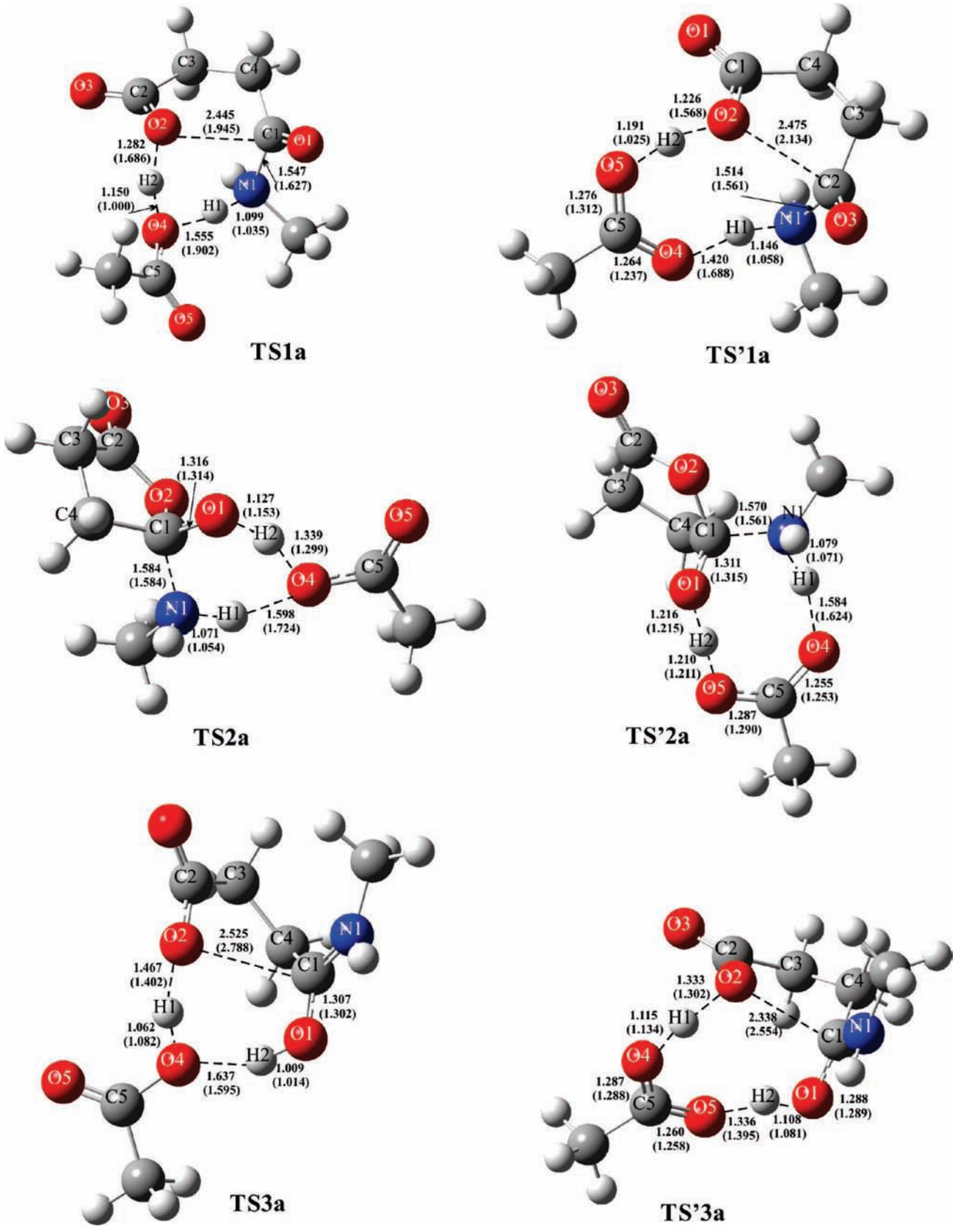

Figure 4. Geometrical parameters of transition states along the concerted and stepwise pathways for the acid catalyzed aminolysis of succinic anhydride optimized at the B3LYP/6−31G(d) and PCM/B3LYP/6−31G(d) (in parentheses) levels of theory.

forms a typical O1···H1 hydrogen bond with the carbonyl oxygen atom from the anhydride molecule, having an equilibrium distance of 1.967 Å at B3LYP/6−311++G(d,p) level of theory and a N2···H1 hydrogen bond (1.247 Å) with the nucleophilic methylamine molecule. The prereactive complex transforms through **TS2b** to the stable intermediate (Figure 2). The catalytic methylamine molecule is combined with this intermediate by an O1H2···N2 hydrogen bond (1.774 Å). The breaking of the

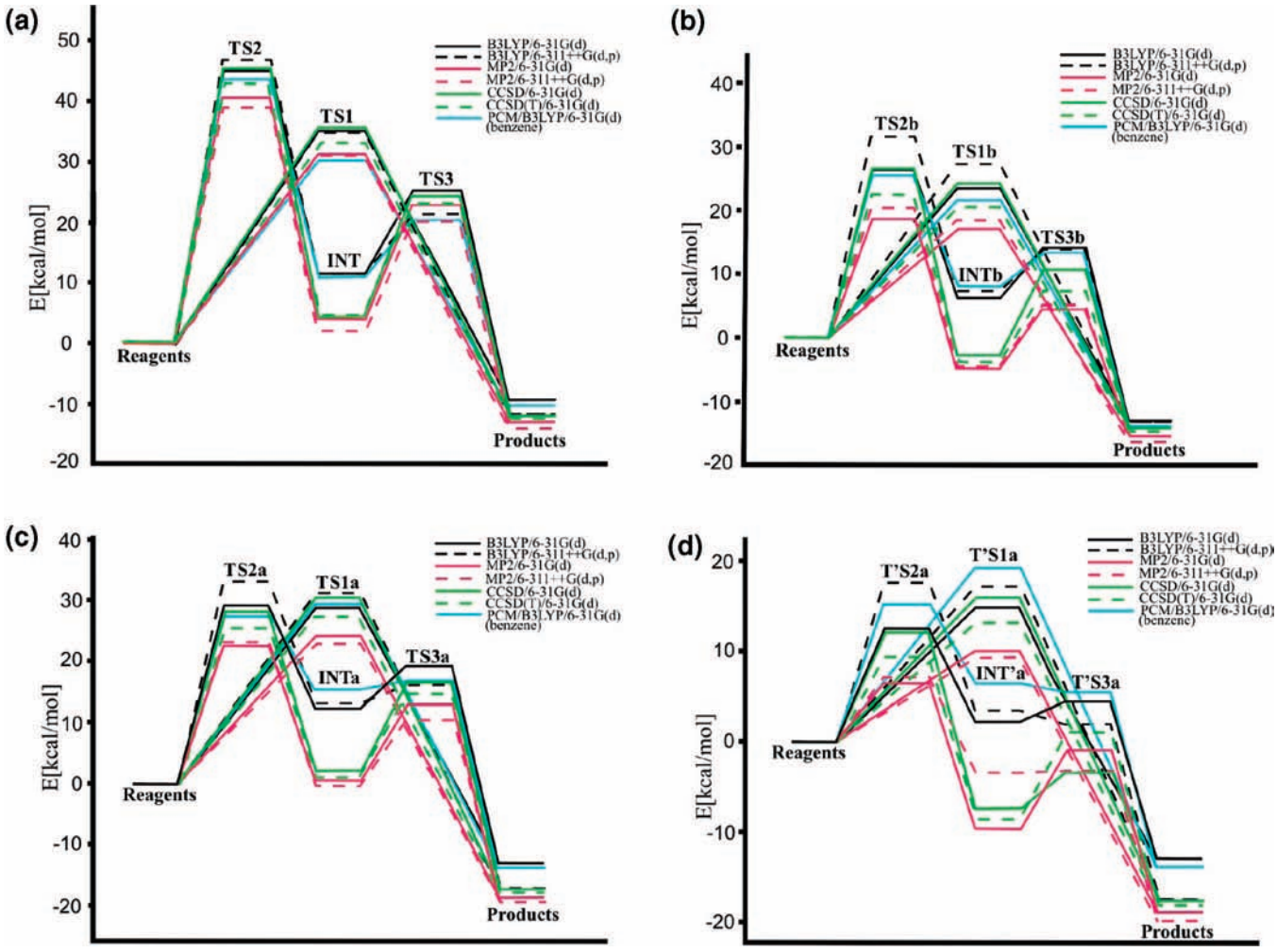

Figure 5. Energy diagrams along the concerted and stepwise pathways for the uncatayzed (a), base catalyzed (b), acid catalyzed (c,d) aminolysis of succinic anhydride.

C1−O2 single bond and the restoration of the C1═O1 double bond occur after the intermediate and a methylamine molecule are preorganized to facilitate the proton transfer process from C1−O1 trough **TS3b**. It is accompanied by the transfer of protons, which is represented by the main component of the vibrational transition vector of **TS3b** (see Supporting Information).

General Acid Catalysis. As we noticed earlier, bifunctional catalysis with a carboxylic acid arises together with the amide from the reaction between the anhydride and the amine. In contrast to aqueous solutions where dissociated acid may neutralize the nucleophilicity of amine, in benzene solution, an acid does not dissociate. So, in this study, we consider the acid as a neutral molecule which participates in the proton transfer processes to catalyze the aminolysis reaction. Let us discuss one of the acid catalyzed mechanisms, the concerted pathway, which is a one-step reaction where all of the bond-forming and bond-breaking processes occur simultaneously. (Scheme 3a). There could be two different transition states, corresponding to the different orientation of the acetic acid with respect to the succinic anhydride.

The transition state **TS1a** should involve simultaneous creation of a C2−N1 bond (1.537 Å at B3LYP/6−311++G(d,p) level of computations), cleavage of C2−O2 single bond in the anhydride (2.562 Å), and migration of two protons (H1 and H2) in the same manner as for the process catalyzed by the second methylamine molecule (Figure 4). The only difference between these processes is that a consecutive proton transfer takes place in the base catalyzed pathway, while the transition vector of the acid-catalyzed concerted transition state **TS1a** corresponds to the simultaneous motion of protons (see Supporting Information).

Also, the general-acid catalyzed reaction can involve the concerted transition state **TS′1a** which proceeds to amide. The transition vector of the **TS′1a** (see Supporting Information) corresponds to partial formation of a C2−N1 bond (1.512 Å in **TS′1a** compared with 1.354 Å in the product at B3LYP/6−311++G(d,p) level of computations), and significant extension of the C2−O2 single bond (2.527 Å in **TS′1a** and 1.389 Å in the succinic anhydride; Figure 4). It is also necessary to state that in this case the proton H1 migrates from the N1 atom of the attacking nucleofile to the carbonyl oxygen O4 atom of the catalytic acid molecule while H2 migrates from the oxygen O5 of the hydroxyl group of the acetic acid to the oxygen O2 of the anhydride. The optimized structures of the transition states along the concerted mechanism are shown in Figure 4.

As in the case of the concerted mechanism, in the neutral stepwise pathway of the acid-catalyzed aminolysis, two ways of catalysis by acetic acid are possible. These two attacks give rise to two similar pathways with distinct sets of transition states with the same product of reaction.

In the fist pathway, the reaction proceeds through an addition/elimination mechanism exactly as in the base-catalyzed stepwise mechanism (Scheme 3a). This bifunctional catalysis involves

TABLE 2: Values of Zero-Point Corrected Activation Energy ($\Delta E^{\ddagger}$), Enthalpy ($\Delta H^{\ddagger}$), Gibbs Free Energies ($\Delta G^{\ddagger}$, kcal/mol) and Entropy ($\Delta S^{\ddagger}$, cal/(mol·K)) for the Concerted and Stepwise Mechanisms of Acid Catalyzed Aminolysis of Succinic Anhydride by Methylamine

		Stepwise mechanism				Stepwise mechanism	
Computational level		Concerted mechanism[a] (Reactants→TS1a)	Step I[a] (Reactants→TS2a)	Step II (Intermediate→TS3a)	Concerted mechanism[a] (Reactants→TS'1a)	Step I[a] (Reactants→TS'2a)	Step II (Intermediate→TS'3a)
B3LYP/6−31G(d)	$\Delta E^{\ddagger}$	8.55	7.91	11.12	−4.96	−8.32	5.95
	$\Delta H^{\ddagger}$	9.09	7.46	12.33	−4.50	−8.39	7.17
	$\Delta S^{\ddagger}$	−65.12	−72.39	18.13	−64.68	−70.08	16.67
	$\Delta G^{\ddagger}$	28.51	29.05	6.93	14.78	12.51	2.21
	$\Delta\Delta^{b}$	23.75	24.93	−0.39	23.53	24.62	0.05
B3LYP/6−311++G(d, p)	$\Delta E^{\ddagger}$	11.02	11.83	7.16	−2.54	−3.17	2.21
	$\Delta G^{\ddagger c}$	30.98	32.97	2.98	17.20	17.66	−1.54
MP2/6−31G(d)// B3LYP/6−311++G(d, p)	$\Delta E^{\ddagger}$	4.09	1.31	16.23	−9.80	−14.45	12.49
	$\Delta G^{\ddagger c}$	24.05	22.46	12.44	9.94	6.38	8.75
MP2/6−311++G(d, p)// B3LYP/6−311++G(d, p)	$\Delta E^{\ddagger}$	2.80	1.77	14.92	−10.48	−13.77	9.47
	$\Delta G^{\ddagger c}$	22.76	22.92	10.73	9.26	7.06	5.73
CCSD/6−31G(d)// B3LYP/6−311++G(d, p)	$\Delta E^{\ddagger}$	10.19	6.77	18.63	−3.71	−8.80	14.59
	$\Delta G^{\ddagger c}$	30.15	27.91	14.45	16.03	12.03	10.84
CCSD(T)/6−31G(d)// B3LYP/6−311++G(d, p)	$\Delta E^{\ddagger}$	7.21	4.17	17.63	−6.67	−11.51	13.40
	$\Delta G^{\ddagger c}$	27.17	25.31	13.45	13.06	9.33	9.65
PCM/B3LYP/6−31G(d)	$\Delta E^{\ddagger}$	6.01	5.06	8.69	−4.45	−7.50	8.05
	$\Delta H^{\ddagger}$	10.30	7.37	7.41	−0.40	−5.50	4.56
	$\Delta S^{\ddagger}$	−63.53	−66.47	19.76	−65.97	−69.33	18.83
	$\Delta G^{\ddagger}$	29.25	27.19	1.53	19.27	15.17	−1.05

[a] Activation parameters have been calculated relative to isolated reactants. [b] ΔΔ−The differences between $\Delta E^{\ddagger}$ and $\Delta G^{\ddagger}$ were derived with the B3LYP/6−311G(d) method and applied to all computational methods. [c] The zero-point corrections as well as the thermal and entropic contributions to the free energies were taken from the B3LYP/6−31G(d) frequency calculations (ΔΔ).

the transfer of two protons (H1 from N1 atom to O4 atom of the acetic acid and H2 from the O4 atom of the acid to the O1 of the anhydride) as well as N1−C1 bond formation in the first step (Figure 4, **TS2a**) that gives the stable intermediate and the isomer of the catalyst in a single step, as shown in Scheme 3.

The intermediate converts to the final product via the breaking of the O2−C1 bond and proton transfers: H1, from O4 atom of the acid to the O2 atom of the anhydride and H2, from the O1 atom to O4 atom of the acid (Figure 4, **TS3a**).

The first transition state along the reaction coordinate with another orientation of the acetic acid with respect to methylamine molecule is **TS′2a** (Figure 4), which corresponds to the C1−N1 formation process as well as proton transfers, and possesses a tetrahedral carbon atom (Scheme 3b). In particular, the transfer of the H2 proton increases the negative charge on the carbonyl oxygen atom O1 of the succinic anhydride and increases basicity on the other site of the catalyst, so it can facilitate the attack of methylamine by H1 proton abstraction. Overcoming this transition state, one is led to the stable intermediate which converts to the product of reaction through the transition state **TS′3a** corresponding to the C1−O2 bond cleavage. At this transition state, proton H2 is removed from O1 oxygen atom to O5 atom of the acetic acid as proton H1 attacks the O2 atom to give the product directly.

Energetics of the Aminolysis Reaction. The calculated values of the activation energy ($\Delta E^{\ddagger}$), enthalpy ($\Delta H^{\ddagger}$), entropy ($\Delta S^{\ddagger}$), and activation Gibbs free energy ($\Delta G^{\ddagger}$) relative to the reactants for the fully optimized critical structures along both concerted and stepwise pathways are given in Table 1 and Table 2. The relative Gibbs free energies of the structures with respect to reactants are schematically represented in Figure 5.

The activation barriers along both concerted and stepwise pathways for the uncatalyzed and base catalyzed aminolysis are given in Table 1. It is important to note that the presence of the second methylamine molecule decreases the values of activation $\Delta E^{\ddagger}$ and $\Delta H^{\ddagger}$ by ≈20 kcal/mol. Because of a significant contribution of entropic factor, the $\Delta G^{\ddagger}$ decreases by ≈30 kcal/mol. Calculations reveal the concerted mechanism to be more favorable than the stepwise pathway either for the uncatalyzed process or for the base catalyzed one (Figure 5a,b). The first stage of the stepwise mechanism is rate-determining in both cases.

These theoretical findings concerning the structures of the transition states, the intermediate, the reactant, and the product of the uncatalyzed and base catalyzed reaction are similar to findings of Ilieva and co-workers for the aminolysis of methyl formate with ammonia.[13] While for ester aminolysis, the B3LYP/6−31G(d) calculations predict the stepwise mechanism to be more favorable than the concerted pathway (38.1 kcal/mol for the rate-determining second stage of the stepwise pathway in comparison with 40.1 kcal/mol for the concerted mechanism).[13] A similar transition state with another form of proton transfer was found by Kruger[25] for concerted aminolysis of acetic anhydride with methylamine with calculations in the gas phase using RHF, B3LYP, and MP2 levels of theory with the 6−31+G(d, p) basis set.

The mechanisms of acid catalysis including only the hydroxyl group of the acetic acid (**TS1a** for concerted mechanism, **TS2a** and **TS3a** for the stepwise one) show a similar energetic picture in comparison with the base catalyzed pathways (**TS1b**, **TS2b**, and **TS3b**, respectively; Figure 5b,c). The only difference is some preference of the stepwise mechanism for this type of catalysis obtained using MP2, CCSD, and CCSD(T) levels of theory.

The comparison of the energetic characteristics for the different types of acid orientation for acid catalyzed aminolysis reaction is of interest (Figure 5c,d). Computational data for the reaction at the same level/basis are available (Table 2). Bifunctional acid catalysis where two oxygen atoms of the acetic acid participate in the proton transfer processes (**TS′1a**, **TS′2a**, and **TS′3a**) was found more favorable in comparison with catalysis including only the hydroxyl group of the acetic acid. Involving the carboxylic group of the acetic acid to catalytic process leads to a decrease in the $\Delta G^{\ddagger}$ value by 13.78 kcal/mol for the concerted pathway (**TS′1a**) and 15.31 kcal/mol (first step, **TS′2a**) and 4.52 kcal/mol (second step, **TS′3a**) for the stepwise process compared with the values for the acid catalyzed aminolysis including one oxygen atom of the acetic acid (**TS1a**, **TS2a**, and **TS3a**, respectively) at the B3LYP/6−311++G(d,p) level of theory. The energy barriers calculated for the first step of the stepwise mechanism are usually higher than those for the second step (except MP2/6−31G(d) and CCSD(T)/6−31G(d) methods). The results reveal the stepwise mechanism is more favorable than the concerted mechanism with a small energy difference. The only exception is calculation at the B3LYP level in the gas phase where concerted mechanism was predicted to be more favorable in some cases (see Table 2).

In this work, we compared the activation energies of uncatalyzed and catalyzed aminolysis. The catalytic role of the second methylamine or the acetic acid molecule affects mostly the proton-transfer processes and the forming of six- or eight-membered rings in the transition state structures which are more stable if compared with four-membered rings in the case of uncatalyzed aminolysis. Base catalysis with another molecule of the reacting amine is considerably less effective than acid catalysis. It should be noticed that consideration of the influence of solvent does not make significant changes into the energetic profiles for the aminolysis reaction of succinic anhydride.

These results are in the agreement with the experimental investigations of the aminolysis reaction in benzene between benzylamine and succinic anhydride performed by Smagowski and Bartnicka[29] which confirm the existence and preferable role of the acid catalysis in the aminolysis reaction.

Conclusions

We have carried out a series of first-principle calculations for the possible reaction pathways of succinic anhydride with methylamine in the gas phase and in solution. The convergence/accuracy of these calculations has been estimated theoretically by comparing a variety of calculation methods using different basis sets. For the aminolysis of cyclic anhydride, the present calculations provide the first quantitative theoretical results for the reaction pathways and for the energy barriers.

Two competing reaction pathways, the concerted process and the two-step stepwise pathway, were found and theoretically confirmed for the studied reaction. The results obtained reveal that both mechanisms involve proton transfers. The energy barriers calculated for the first step of the stepwise process for catalyzed and uncatalyzed aminolysis (the formation of the tetrahedral intermediate) are usually higher than those for the second step (the decomposition of the tetrahedral intermediate to the products). The structure and transition vectors of the transition states indicate that the catalytic role of methylamine and acetic acid is executed by facilitating the proton transfer processes and by decreasing all energy barriers. The only difference between these processes is that a consecutive proton transfers take place in the base catalyzed pathways, while the transition vectors of the acid-catalyzed transition states correspond to the simultaneous motion of protons.

In the acid catalyzed aminolysis reaction, there could be two different types of transition states, corresponding to the different orientation of the acetic acid with respect to the succinic anhydride. The forming eight-membered rings in the transition state structures were found more stable if compare with the six-membered rings. The results show that the most favorable pathway of the reaction is through the bifunctional acid catalyzed stepwise mechanism. The presence of the aprotic solvent benzene lowers all energy barriers.

Acknowledgment. This paper is dedicated to Professor Liliya Kasyan on the occasion of her 70th birthday. This work was supported in part by the National Science Foundation through RISE Grant HRD-0401730. We thank the Mississippi Center for Supercomputer Research for a generous allotment of computer time.

Supporting Information Available: Cartesian coordinates for fully optimized geometries; tables of total electronic energies, enthalpy, entropy, Gibbs free energies and zero-point corrections; the reaction-coordinate vectors of transition states. This material is available free of charge via the Internet at http://pubs.acs.org.

References and Notes

(1) Bunnett, J. F.; Davis, G. T. *J. Am. Chem. Soc.* **1960**, *82*, 665.
(2) Jencks, W. P.; Carriuolo, J. *J. Am. Chem. Soc.* **1960**, *82*, 675.
(3) Blackburn, G. M.; Jencks, W. P. *J. Am. Chem. Soc.* **1968**, *90*, 2638.
(4) Jencks, W. P.; Gilchrist, M. *J. Am. Chem. Soc.* **1966**, *88*, 104.
(5) Bruice, T. C.; Mayahi, M. F. *J. Am. Chem. Soc.* **1960**, *82*, 3067.
(6) Bruice, T. C.; Donzel, A.; Huffman, R. W.; Butler, A. R. *J. Am. Chem. Soc.* **1967**, *89*, 2106.
(7) Rogers, G. A.; Bruice, T. C. *J. Am. Chem. Soc.* **1973**, *95*, 4452.
(8) Rogers, G. A.; Bruice, T. C. *J. Am. Chem. Soc.* **1974**, *96*, 2473.
(9) Bruice, T. C.; Benkovic, S. J. *J. Bioorganic Mechanisms*; W.A. Benjamin Inc.: New York, 1966; Vol. 1.
(10) Jencks, W. P. *Catalysis in Chemistry and Enzymology*; McGraw-Hill: New York, 1969.
(11) Williams, A. *Acc. Chem. Res.* **1989**, *22*, 387.
(12) Yang, W.; Drueckhammer, D. G. *Org. Lett.* **2000**, *2*, 4133.
(13) Ilieva, S.; Galabov, B.; Musaev, D. G.; Morokuma, K.; Schaefer, H. F., III *J. Org. Chem.* **2003**, *68*, 1496.
(14) Cox, M. M.; Jencks, W. P. *J. Am. Chem. Soc.* **1981**, *103*, 572.
(15) Satterthwait, A. C.; Jencks, W. P. *J. Am. Chem. Soc.* **1974**, *96*, 7018.
(16) Fox, J. P.; Page, M. I.; Satterthwait, A. C.; Jencks, W. P. *J. Am. Chem. Soc.* **1972**, *94*, 4731.
(17) Yang, C. C.; Jencks, W. P. *J. Am. Chem. Soc.* **1988**, *110*, 2972.
(18) O'Hair, R. A. J.; Androutsopoulos, N. K. *Org. Lett.* **2000**, *2*, 2567.
(19) Kim, C. K.; Li, H. G.; Lee, H. W.; Sohn, C. K.; Chun, Y. I.; Lee, I. *J. Phys.Chem. A* **2000**, *104*, 4069.
(20) Zipse, H.; Wang, L.; Houk, K. N. *Liebigs Ann.* **1996**, 1511.
(21) Wang, L.; Zipse, H. *Liebigs Ann.* **1996**, 1501.
(22) Oie, T.; Loew, G. H.; Burt, S. K.; Binkley, J. S.; McErloy, R. D. *J. Am. Chem. Soc.* **1982**, *104*, 6169.
(23) Singleton, D. A.; Merrigan, S. R. *J. Am. Chem. Soc.* **2000**, *122*, 11035.
(24) Marlier, J. F.; Haptonsall, B. A.; Johnson, A. J.; Sacksteder, K. A. *J. Am. Chem. Soc.* **1997**, *119*, 8838.
(25) Kruger, H. G. *J. Mol. Struct.(Theochem)* **2002**, *577*, 281.
(26) Yamabe, S.; Ishikawa, T. *J. Org. Chem.* **1997**, *62*, 7049.
(27) Kasyan, A. O.; Krischik, O. V.; Krasnovskaya, O.Yu.; Kasyan, L. I. *Rus. J.Org.Chem.* **1998**, *12*, 1802.
(28) Bartnicka, H.; Smagowski, H. *Pol. J. Chem.* **1992**, *66*, 1277.
(29) Bartnicka, H.; Smagowski, H. *Pol. J. Chem.* **1992**, *66*, 1295.
(30) Patent No.: US 6.479.264 B1, Nov. 12, 2002..
(31) Scott, A. P.; Radom, L. *J. Phys. Chem.* **1996**, *100*, 16502–16513.
(32) For conversion from 1 atm standard state to 1 mol/L standard state, the following contributions need to be added to standard enthalpy, entropy, and Gibbs free energy: $-RT$, $-R-R\ln R'T$, and $RT\ln R'T$, where R' is the value of R in L·atm/mol·K (ref 37). For a reaction with A + B = C stoichiometry (such as the uncatalyzed aminolysis mechanism, Figure 1), the corrections for $\Delta H^{\ddagger}$, $\Delta S^{\ddagger}$, and $\Delta G^{\ddagger}$ are RT, $R + R\ln R'T$, and $RT\ln R'T$. At 298 K, the corrections amount to 0.59 and −1.90 kcal/mol for $\Delta H^{\ddagger}$ and $\Delta G^{\ddagger}$ and +8.34 eu for $\Delta S^{\ddagger}$ (ref 38). For a reaction with A + B + C = D stoichiometry (such as the aminolysis mechanism, catalyzed by second methylamine, Figure 4), the corrections for $\Delta H^{\ddagger}$, $\Delta S^{\ddagger}$, and $\Delta G^{\ddagger}$ are $2RT$,

$2(R + R \ln R'T')$, and $2RT \ln R'T'$. At 298 K, the corrections amount to 1.18 and −3.79 kcal/mol for $\Delta H^{\ddagger}$ and $\Delta G^{\ddagger}$ and +16.68 eu for $\Delta S^{\ddagger}$.

(33) (a) Fukui, K. *J. Phys. Chem.* **1970**, *74*, 4161. (b) Fukui, K. *Acc. Chem. Res.* **1981**, *14*, 363.

(34) (a) Gonzalez, C.; Schlegel, H. B. *J. Chem. Phys.* **1989**, *90*, 2154. (b) Gonzalez, C.; Schlegel, H. B. *J. Chem. Phys.* **1990**, *94*, 5523.

(35) (a) Deng, L.; Ziegler, T.; Fan, L. *J. Chem. Phys.* **1993**, *99*, 3822. (b) Deng, L.; Ziegler, T. *Int. J. Quantum Chem.* **1994**, *52*, 731.

(36) Miertus, S.; Scrocco, E.; Tomasi, J. *J. Chem. Phys.* **1981**, *55*, 117.

(37) Benson, S. *Thermochemical Kinetics*; Wiley: New York, 1968; p 8.

(38) Rastelli, A.; Bagatti, M.; Gandolfi, R. *J. Am. Chem. Soc.* **1995**, *117*, 4965.

JP7102897